Figure 2. Stereoview of the unit cell of PcCo(py)SCN·CHCl₃ (3).
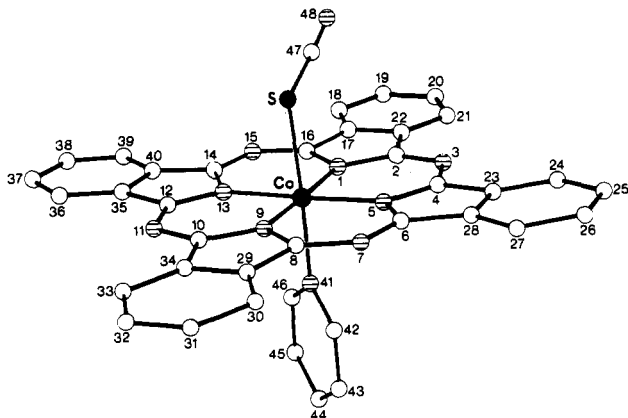

Figure 3. Molecular structure and atom-labeling scheme of PcCo(py)-SCN·CHCl₃ (3).

valence frequencies due to their monomeric metal–N-bonded structure (Table IV).

Powder diffraction data of **2** and [PcMSCN]$_n$ (M = Fe,[44] Mn[45]), which were shown to exhibit a bridged structure, are almost identical and give evidence for an isostructural lattice. The EPR spectrum of [PcCoSCN]$_n$ (**2**) shows no Co(II) absorption.

The dc dark powder conductivities of compounds **1–4** and **7** are given in Table V. The conductivity of [PcCoSCN]$_n$ (**2**) is only slightly lower than the value of [PcCoCN]$_n$ (σ_{RT} = 2 × 10⁻² S/cm)². A similar observation was made in the [PcFeL]$_n$ series (L = CN, SCN).[24,44] The reason for that slight decrease could

be the larger interplanar distance of the phthalocyanine ring systems or a more angular polymer chain in [PcCoSCN]$_n$ (**2**) in comparison with that of [PcCoCN]$_n$² because of the electron configuration of the sulfur atom. The influence of the linearity of the polymer chain on the conductive behavior was shown recently in the case of [PcRu(*p*-dib)]$_n$⁶ and [PcRu(*m*-dib)]$_n$.[29] The conductivity of [PcRu(*m*-dib)]$_n$ is 1 order of magnitude lower than that of [PcRu(*p*-dib)]$_n$.

As in the case of **1** and **5**, the ¹H NMR spectra of PcCo-(py)SCN·CHCl₃ (**3**), TBA[(TBP)Co(NCS)₂] (**6**), and (TBP)-CoNCS (**7**) give evidence for two isomeric complexes in solution. In the case of **3** the metal–S-bonded species predominates; the ratio of isothiocyanate to thiocyanate complex is about 1:4. The AA′XX′ spin system and the signals of the pyridine ligand of each isomer have slightly different chemical shifts. The spectra of **6** and **7** show a higher concentration of the metal–N-bonded isomers.

In the solid state only the S-bonded isomer of **3** is observed. The conclusion drawn from the IR data was proven to be correct by X-ray analysis of PcCo(py)SCN·CHCl₃ (**3**) (Figures 2 and 3).

According to X-ray data the central Co atom lies slightly above the almost planar Pc ring system in the direction of the pyridine ligand. The Co–S distance of 226.9 (2) pm and the Co–S–C angle of 106.9 (2)° are in the range of those observed in other Co-(III)–S-bonded species.[46] The thiocyanate group is oriented in the direction of an isoindole ring, while the plane of the pyridine ligand is perpendicular to the phthalocyanine core, passing through the aza bridges of the macrocycle[47] (Figure 3).

Acknowledgment. We thank the Stiftung Volkswagenwerk for financial support.

(44) Keppeler, U. Ph.D. Thesis, University of Tübingen, Tübingen, West Germany, 1985.

(45) Datz, A. Ph.D. Thesis, University of Tübingen, Tübingen, West Germany, 1985.

(46) Snow, M. R.; Boomsa, R. F. *Acta Crystallogr., Sect. B: Struct. Crystallogr. Cryst. Chem.* **1972**, *B28*, 1908.

(47) Collins, D. M.; Countryman, R.; Hoard, J. L. *J. Am. Chem. Soc.* **1972**, *94*, 2066.

Contribution from the Chemistry Department,
The Ohio State University, Columbus, Ohio 43210

Steric Control of Electronic Effects in Diacetylated Nickel(II) Schiff Base Complexes

Kenneth A. Goldsby, Alan J. Jircitano, David M. Minahan, Dorai Ramprasad, and Daryle H. Busch*

X-ray structural analysis, electrochemistry, ¹³C NMR spectroscopy, and infrared spectroscopy of the diacetylated Schiff base complexes [Ni(Me₂Ac₂H₂malen)] and [Ni(Me₂Ac₂Me₂malen)] are reported. Differences in the number of methyl groups on the chelate backbone (two for [Ni(Me₂Ac₂H₂malen)], four for [Ni(Me₂Ac₂Me₂malen)]) cause the acetyl groups to be rotated out of the NiN₂O₂ plane by 16.8 and 58.2°, respectively. Electrochemical measurements on the diacetylated and analogous deacetylated complexes show that delocalization effects from the acetyl groups have been decreased by the rotating of the acetyl groups out of the chelate plane. This interpretation is supported by ¹³C NMR and infrared spectroscopic measurements. As such, the use of steric effects to regulate electronic effects has been demonstrated. [Ni(Me₂Ac₂H₂malen)] crystallized in the monoclinic system ($P2_1/c$) with unit cell dimensions a = 14.686 (2) Å, b = 17.734 (3) Å, c = 11.412 (1) Å, β = 101.16 (1)°, and Z = 8; R = 0.049 and R_w = 0.054 for 2730 observed reflections. [Ni(Me₂Ac₂Me₂malen)] crystallized in the monoclinic system ($C2/c$) with unit cell dimensions a = 7.689 (2) Å, b = 8.686 (2) Å, c = 25.579 (9) Å, β = 103.84 (3)°, and Z = 4; R = 0.042 and R_w = 0.042 for 1370 observed reflections.

Introduction

We have previously reported the reversible binding of dioxygen to a new family of cobalt(II) and iron(II) lacunar complexes based on the cyclidene macrocycle.[1–3] The precursor macrocycle, which

was first synthesized by Jager,[4] is formed in a template reaction between a nickel(II) complex of the linear tetradentate ligand

(1) Stevens, J. C.; Busch, D. H. *J. Am. Chem. Soc.* **1980**, *102*, 3285–3287.

shown in structure I (R is ethylene or *n*-propylene) and an ap-

I
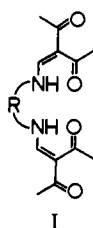
propriate diamine.[4-6] Nickel(II) remains in the macrocycle until the ligand has been modified to give the desired lacunar complex, at which time the nickel(II) is removed and cobalt(II) or iron(II) is inserted.

Recently, Okawa and co-workers have shown that cobalt(II) complexes of the linear tetradentate ligand shown in structure I are themselves reversible dioxygen carriers at room temperature.[7] Furthermore, in addition to showing a high affinity for dioxygen, these complexes display good stability with regard to autoxidation. The high affinity for dioxygen and resistance toward autoxidation relative to the case for other cobalt(II) Schiff base complexes were attributed to the electron-withdrawing effects of the acetyl groups.[7,8]

In an effort to understand the special role, if any, of the acetyl groups in these complexes, we have structurally characterized the parent nickel(II) complex shown in structure II, as well as the analogous complex formed by the diacetylation of [Ni-(Me_2H_2Me_2malen)][9] (structure III). It was our hope that the


II   III
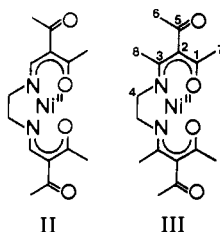
added methyl groups in structure III would introduce sufficient steric bulk in the vicinity of the acetyl groups to alter their orientations relative to the NiN_2O_2 plane and hence allow one to distinguish between resonance and inductive effects arising from the acetyl groups. The deacetylated complexes (structures IV and V) have also been synthesized and studied, so that the inductive

Table I. Crystal Data for [Ni(Me_2Ac_2H_2malen)] and [Ni(Me_2Ac_2Me_2malen)]

complex	[Ni(Me_2Ac_2H_2malen)]	[Ni(Me_2Ac_2Me_2malen)]
formula	$NiC_{14}H_{18}N_2O_4$	$NiC_{16}H_{22}N_2O_4$
system	monoclinic	monoclinic
space group	$P2_1/c$	$C2/c$
a, Å	14.686 (2)[a]	7.689 (2)
b, Å	17.734 (3)[a]	8.686 (2)
c, Å	11.412 (1)[a]	25.579 (9)
α, deg	90	90
β, deg	101.16 (1)	103.84 (3)
δ, deg	90	90
V, Å^3	2916 (1)	1659 (2)
Z	8	4
$F(000)$	1408.0	768.0
D_{calcd}, g cm^{-3}	1.535	1.462
D_{obsd}, g cm^{-3} [b]	1.52 (1)	1.42 (1)
$\mu_{Mo K\alpha}$, cm^{-1}	13.28	11.90
λ, Å	0.710 69	0.710 69
T, °C	20	20

[a]Two molecules per asymmetric unit. [b]Determined by flotation in heptane/CCl_4.

effects of the added methyl groups may be considered separately and factored out.

IV   V
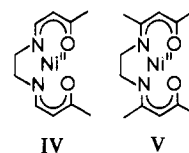
Experimental Section

Materials. Reagent grade solvents and chemicals were used in the syntheses of the nickel(II) complexes. Solvents were dried by following recommended procedures[10] and distilled under nitrogen before use. Electrochemical grade tetra-*n*-butylammonium tetrafluoroborate (TBAT) was purchased from Southwestern Analytical Co. and used as received.

Syntheses. The complexes [Ni(Me_2H_2H_2malen)],[4] [Ni-(Me_2H_2Me_2malen)],[11] and [Ni(Me_2Ac_2H_2malen)][6] were synthesized by literature methods. Rigorous drying of triethylamine, acetyl chloride, and all solvents was required to optimize preparation of the nickel(II) complexes.

[3,3'-Diacetyl-4,4'-(1,2-ethanediyldinitrilo-κ^2N)bis(2-pentanonato-κ^2O)]nickel(II), [Ni(Me_2Ac_2Me_2malen)]. [Ni(Me_2H_2Me_2malen)] (5 g, 0.018 mol) and triethylamine (3.6 g, 0.036 mol) were dissolved in 250 mL of dry 1,2-dichloroethane and heated to reflux. A solution of acetyl chloride (3 g, 0.036 mol) in 100 mL of 1,2-dichloroethane was added dropwise to the refluxing solution over a period of 1 h. The solution was heated at reflux for a further 48 h, filtered to remove the triethylamine hydrochloride produced during the course of the reaction, and reduced in volume to roughly 30 mL by rotary evaporation. The solution was passed down a column of neutral alumina packed under 1,2-dichloroethane with 1,2-dichloroethane as eluent. The first, fast-moving red band was collected and reduced in volume by rotary evaporation. The brick red product was precipitated by the addition of diethyl ether and recrystallized from dichloromethane/heptane. Anal. Calcd for $NiC_{16}H_{22}N_2O_4 \cdot {}^1/_2H_2O$: C, 51.36; H, 6.21; N, 7.49. Found: C, 51.44, 51.74; H, 6.36, 6.47; N, 7.90, 7.29. X-ray-quality crystals were obtained by slow evaporation from ethanol, as noted below.

Physical Measurements. Infrared spectra were recorded on KBr pellets on a Perkin-Elmer 457 grating infrared spectrometer. ^{13}C NMR spectra were recorded on a Bruker WP-80 or HX90 spectrometer in the Fourier transform mode with broad-band proton decoupling.

Electrochemical measurements were performed by using a Princeton Applied Research Model 173 potentiostat equipped with a Model 175 linear programmer. Current vs. potential curves were measured on a Houston Instruments Model 2000 XY recorder. Measurements were carried out at a platinum disk in 0.1 M $TBAT/CH_3CN$, and the potentials were measured vs. a $Ag/0.1$ M $AgNO_3/CH_3CN$ reference

(2) (a) Herron, N.; Busch, D. H. *J. Am. Chem. Soc.* **1981**, *103*, 1236–1237. (b) Herron, N.; Cameron, J. H.; Near, G. L.; Busch, D. H. *J. Am. Chem. Soc.* **1983**, *105*, 298–301. (c) Herron, N.; Zimmer, L. L.; Grzybowski, J. J.; Olszanski, D. J.; Jackels, S. C.; Callahan, R. W.; Cameron, J. H.; Christoph, G. G.; Busch, D. H. *J. Am. Chem. Soc.* **1983**, *105*, 6585–6596.

(3) Goldsby, K. A.; Beato, B. D.; Busch, D. H. *Inorg. Chem.* **1986**, *25*, 2342.

(4) Wolf, L.; Jager, E. *Z. Anorg. Allg. Chem.* **1966**, *346*, 76.

(5) (a) Jager, E. *Z. Chem.* **1968**, *8*, 30. (b) Jager, E. *Z. Chem.* **1968**, *8*, 392.

(6) Riley, D. P.; Busch, D. H. *Inorg. Synth.* **1978**, *18*, 36–44.

(7) Kubokura, K.; Okawa, H.; Kida, S. *Bull. Chem. Soc. Jpn.* **1978**, *51*, 2036–2040.

(8) (a) Nishida, Y.; Kida, S.; Cremer, S.; Nakamoto, K. *Inorg. Chim. Acta* **1981**, *49*, 85–89. (b) Nakamoto, K.; Nonaka, Y.; Ishiguro, T.; Urban, M. W.; Suzuki, M.; Kozuka, M.; Nishida, Y.; Kida, S. *J. Am. Chem. Soc.* **1982**, *104*, 3386–3391.

(9) The abbreviations used here refer to the structure below, where Me is methyl, Ac is acetyl, and en is ethylene:
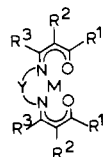
[M(R$^1_2$R$^2_2$R$^3_2$malY)]

(10) Perrin, D. D.; Armarego, W. L. F. *Purification of Laboratory Chemicals*, 2nd ed.; Pergamon: Oxford, 1980.

(11) McCarthy, P. J.; Hovey, R. J.; Veno, K.; Martell, A. E. *J. Am. Chem. Soc.* **1955**, *77*, 5820.

electrode. Half-wave potentials were determined as the average of the peak cathodic and peak anodic potentials; i.e., $E_{1/2} = (E_{p,a} + E_{p,c})/2$. All measurements were performed in a glovebox under an atmosphere of dry nitrogen.

Elemental analysis was performed by Galbraith, Inc., Knoxville, TN.

Crystal Data. Data were collected with a Syntex P2$_1$ four-circle automated diffractometer.

(a) [Ni(Me$_2$Ac$_2$H$_2$malen)]. Crystals were grown as dark plates, by slow evaporation of an ethanol solution. Crystal data information is given in Table I. Preliminary measurements indicated monoclinic symmetry with systematic absences $h0l$, $l = 2n + 1$, and $0k0$, $k = 2n + 1$, indicative of space group $P2_1/c$. Unit cell parameters were determined by accurate centering of 15 reflections well-distributed in reciprocal space. Data were collected by using the θ–2θ technique, with a variable scan rate ranging from 2.0 to 24.0° min^{-1} in the region $4° < 2\theta < 50°$, depending upon the intensity of a 2-s prescan. The scan range was 1.0° below the Kα_1 peak to 1.0° above Kα_2, with background counts taken with a background-to-scan ratio of 0.5 at the beginning and end of each 2θ scan. A total of 5717 reflections (4519 unique and 2730 with $I > 3\sigma(I)$) were collected and used in the structural determination. Intensities and standard deviations were calculated according to the formula $I = r(S - RB)$ and $I^2 = r^2(S - R^2B)$, respectively, where r is the scan rate in degrees per minute, S is the total scan count, R is the scan-to-background time ratio, and B is the total background count. Six standard reflections monitored every 100 reflections showed only random fluctuations. The data were corrected for background, and Lorentz and polarization factors were applied to obtain structure factors. Wilson's method was used to bring F^2 to a relatively absolute scale. The I^2 values were scaled by increasing the I^2 value obtained from counting statistics by PI^2, where P was chosen as the rms deviation of the standard reflections.

(b) [Ni(Me$_2$Ac$_2$Me$_2$malen)]. Crystals were grown as red plates, by slow evaporation from ethanol. Crystal data information is given in Table I. Preliminary measurements indicated monoclinic symmetry with systematic absences $h0l$, $l = 2n$, and hkl, $h + k = 2n$, indicative of space groups $C2/c$ and Cc. Unit cell parameters were determined by accurate centering of 15 reflections well-distributed in reciprocal space. Data were collected by using the θ–2θ technique, with a variable scan rate ranging from 2.0 to 24.0° min^{-1} in the region $4° < 2\theta < 55°$, depending upon the intensity of a 2-s prescan. The scan range was 1.0° below the Kα_1 peak to 1.0° above Kα_2, with background counts taken with a background-to-scan ratio of 0.5 at the beginning and end of each 2θ scan. A total of 2249 reflections (1793 unique and 1370 with $I > 3\sigma(I)$) were collected and used in the structural determination. The intensities and standard deviations were calculated and treated as described above for [Ni-(Me$_2$Ac$_2$H$_2$malen)].

Solution and Refinement of Structures. For both data sets, the position of the heavy atom was ascertained from a Patterson map, and the positions of the remaining non-hydrogen atoms were revealed by subsequent Fourier maps. Refinement was performed by using full-matrix least-squares techniques, during which the function $\sum(w(|F_o| - |F_c|))^2$ was minimized. The data were weighted according to $1/\sigma_F^2$. Residuals were calculated as $R = \sum(|F_o| - |F_c|)/\sum|F_o|$ and $R_w = (\sum(|F_o| - |F_c|)^2/\sum w|F_o|^2)^{1/2}$. Atomic scattering factors were taken from ref 12 for H, C$_{cov}$, N, O, and Ni. All calculations were carried out on an Amdahl 470/V6 computer in the Computer Center of The Ohio State University with the CRYM[13a] and XRAY72[13b] crystallographic computing systems.

(a) [Ni(Me$_2$Ac$_2$H$_2$malen)]. Isotropic refinement resulted in convergence at $R = 0.088$. At this point, the thermal parameters were allowed to vary anisotropically. Hydrogen atom positions were calculated and were introduced as fixed contributions. Subsequent full-matrix least-squares refinement resulted in convergence at $R = 0.049$ and $R_w = 0.054$. In the final cycle of refinement, no atom shifted by more than 0.45 of its esd. A final difference map was virtually featureless.

(b) [Ni(Me$_2$Ac$_2$Me$_2$malen)]. Isotropic refinement resulted in convergence at $R = 0.136$. At this point, the thermal parameters were allowed to vary anisotropically. Hydrogen atom positions were located from a difference map and were introduced as fixed contributions with 5.0-Å^2 thermal parameters. Subsequent full-matrix least-squares refinement resulted in convergence at $R = 0.042$ and $R_w = 0.042$. In the final cycle of refinement, no atom shifted by more than 0.03 of its esd. A final difference map was featureless.
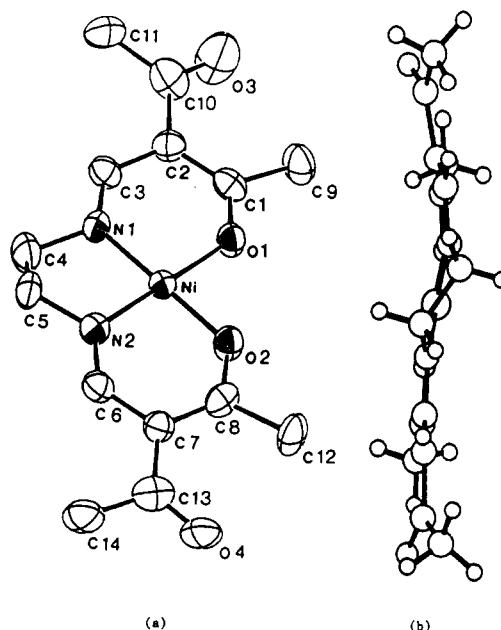
(12) *International Tables for X-ray Crystallography*; Kynoch: Birmingham, England, 1974; Vol. IV.

(13) (a) DuChamp, D. J. *Program and Abstracts*, American Crystallographic Association Meeting, Bozeman, MT, 1964; American Crystallographic Association: Storrs, CT, 1964; Paper B14. This program was modified by G. G. Christoph while at The Ohio State University. (b) Technical Report TR-192; Computer Science Center, University of Maryland: College Park, MD, 1972.

Figure 1. (a) ORTEP drawing for [Ni(Me$_2$Ac$_2$H$_2$malen)].[9] (b) Alternate view of [Ni(Me$_2$Ac$_2$H$_2$malen)].
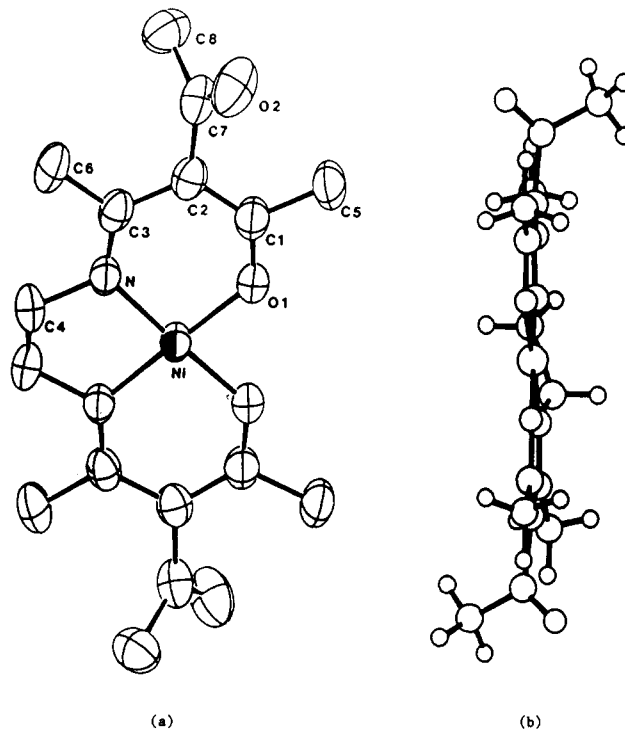
Figure 2. (a) ORTEP drawing for [Ni(Me$_2$Ac$_2$Me$_2$malen)].[9] (b) Alternate view of [Ni(Me$_2$Ac$_2$Me$_2$malen)].

Results

Crystal Structures. Figures 1 and 2 show the molecular structures of the acetylated complexes [Ni(Me$_2$Ac$_2$H$_2$malen)] and [Ni(Me$_2$Ac$_2$Me$_2$malen)], respectively. Final atomic position coordinates are given in Table II, and bond lengths and angles are given in Table III. The individual bond lengths and bond angles are unremarkable. In both complexes, the linear tetradentate ligands form square-planar complexes around nickel(II), and the N$_2$O$_2$ donor atoms are essentially in the same plane as the central Ni^{II} ion. Furthermore, the acetyl groups are nearly planar in both structures, consistent with an sp^2 geometry for the carbonyl carbons. Consequently, one may define an angle that relates the extent to which the acetyl group is rotated out of the NiN$_2$O$_2$ plane.[14]

Table II. Atomic Coordinates

atom	x	y	z
	A. [Ni(Me$_2$Ac$_2$H$_2$malen)]		
Ni1	0.64529 (7)	0.27737 (6)	0.19356 (8)
N11	0.6805 (4)	0.3748 (3)	0.2359 (5)
N21	0.5722 (4)	0.2826 (4)	0.3065 (5)
O11	0.7182 (4)	0.2743 (3)	0.0779 (5)
O21	0.6110 (4)	0.1785 (3)	0.1542 (5)
O31	0.7865 (6)	0.4610 (4)	−0.1066 (5)
O41	0.4494 (5)	0.0372 (4)	0.3270 (6)
C11	0.7517 (5)	0.3283 (4)	0.0283 (6)
C21	0.7466 (5)	0.4044 (4)	0.0638 (6)
C31	0.7167 (5)	0.4215 (4)	0.1722 (6)
C41	0.6544 (6)	0.3979 (4)	0.3485 (7)
C51	0.5625 (6)	0.3607 (4)	0.3506 (8)
C61	0.5311 (5)	0.2287 (4)	0.3487 (7)
C71	0.5278 (6)	0.1523 (4)	0.3072 (7)
C81	0.5666 (6)	0.1332 (4)	0.2084 (7)
C91	0.8002 (6)	0.3054 (5)	−0.0697 (8)
C101	0.7743 (6)	0.4678 (5)	−0.0053 (7)
C111	0.7867 (6)	0.5451 (4)	0.0520 (7)
C121	0.5573 (8)	0.0549 (5)	0.1525 (9)
C131	0.4790 (6)	0.0982 (5)	0.3699 (8)
C141	0.4621 (7)	0.1176 (5)	0.4918 (8)
Ni2	0.88260 (7)	0.47077 (6)	0.44431 (8)
N12	0.9474 (5)	0.3874 (4)	0.5060 (6)
N22	0.8344 (4)	0.4743 (4)	0.5811 (5)
O12	0.9304 (4)	0.4668 (3)	0.3064 (4)
O22	0.8171 (4)	0.5554 (3)	0.3816 (4)
O32	1.0751 (5)	0.2906 (3)	0.1850 (6)
O42	0.6490 (6)	0.6945 (5)	0.5451 (7)
C12	0.9806 (5)	0.4157 (5)	0.2705 (7)
C22	1.0104 (5)	0.3499 (4)	0.3360 (7)
C32	0.9940 (5)	0.3424 (4)	0.4534 (7)
C42	0.9428 (7)	0.3745 (5)	0.6334 (7)
C52	0.8532 (7)	0.4047 (5)	0.6532 (8)
C62	0.7844 (5)	0.5259 (5)	0.6127 (7)
C72	0.7494 (5)	0.5906 (4)	0.5463 (7)
C82	0.7660 (5)	0.5998 (4)	0.4287 (7)
C92	1.0051 (6)	0.4348 (5)	0.1501 (8)
C102	1.0622 (6)	0.2912 (5)	0.2870 (8)
C112	1.1007 (7)	0.2254 (6)	0.3665 (8)
C122	0.7251 (6)	0.6631 (5)	0.3476 (8)
C132	0.6947 (6)	0.6446 (5)	0.5997 (9)
C142	0.6949 (6)	0.6389 (5)	0.7330 (8)
	B. [Ni(Me$_2$Ac$_2$Me$_2$malen)]		
Ni	0.0000 (0)	0.0633 (1)	0.2500 (0)
N	0.0915 (4)	−0.0880 (3)	0.2995 (1)
O1	0.0894 (4)	0.2200 (2)	0.2965 (1)
O2	0.4283 (4)	0.1626 (4)	0.4513 (1)
C1	0.1717 (5)	0.2129 (4)	0.3456 (2)
C2	0.2142 (4)	0.0775 (4)	0.3747 (1)
C3	0.1792 (4)	−0.0712 (4)	0.3492 (1)
C4	0.0770 (6)	−0.2421 (4)	0.2747 (2)
C5	0.2129 (6)	0.3700 (4)	0.3710 (2)
C6	0.2570 (5)	−0.2118 (4)	0.3818 (8)
C7	0.2958 (5)	0.0877 (4)	0.4334 (2)
C8	0.1989 (6)	0.0149 (5)	0.4712 (2)
O11	−0.0849 (5)	0.2200 (4)	0.2035 (2)
N11	−0.0915 (5)	−0.0880 (4)	0.2005 (2)
C41	−0.0770 (5)	−0.2421 (4)	0.2253 (2)

Table III. Bond Lengths (Å) and Bond Angles (deg)

	A. [Ni(Me$_2$Ac$_2$H$_2$malen)]		
Ni–N1	1.841 (05)	C1–C2	1.415 (10)
Ni–N2	1.832 (05)	C1–C9	1.494 (11)
Ni–O1	1.854 (05)	C2–C3	1.423 (09)
Ni–O2	1.855 (05)	C2–C10	1.475 (11)
N1–C3	1.283 (09)	C4–C5	1.507 (10)
N1–C4	1.469 (09)	C6–C7	1.433 (10)
N2–C5	1.490 (10)	C7–C8	1.400 (11)
N2–C6	1.274 (09)	C7–C13	1.464 (11)
O1–C1	1.260 (09)	C8–C12	1.523 (12)
O2–C8	1.269 (09)	C10–C11	1.515 (11)
O3–C10	1.210 (10)	C13–C14	1.500 (13)
O4–C13	1.232 (11)		
N2–Ni–N1	86.6 (3)	C10–C2–C1	122.6 (6)
O1–Ni–N1	92.5 (2)	C10–C2–C3	117.8 (6)
O2–Ni–N1	178.8 (3)	C2–C3–N1	125.9 (7)
O1–Ni–N2	178.6 (3)	C5–C4–N1	106.1 (6)
O2–Ni–N2	92.8 (3)	C4–C5–N2	104.9 (6)
O2–Ni–O1	88.1 (2)	C7–C6–N2	124.9 (7)
C3–N1–Ni	125.7 (5)	C8–C7–C6	120.1 (7)
C4–N1–Ni	112.6 (4)	C13–C7–C6	116.5 (7)
C4–N1–C3	121.5 (6)	C13–C7–C8	123.3 (7)
C5–N2–Ni	113.1 (5)	C7–C8–O2	124.6 (7)
C6–N2–Ni	127.8 (6)	C12–C8–O2	112.7 (7)
C6–N2–C5	119.1 (6)	C12–C8–C7	122.7 (7)
C1–O1–Ni	128.8 (5)	C2–C10–O3	122.8 (8)
C8–O2–Ni	128.4 (5)	C11–C10–O3	118.4 (8)
C2–C1–O1	123.3 (6)	C11–C10–C2	118.8 (7)
C9–C1–O1	114.5 (7)	C7–C13–O4	123.4 (8)
C9–C1–C2	122.2 (6)	C14–C13–O4	117.5 (8)
C3–C2–C1	119.6 (6)	C14–C13–C7	119.2 (7)
	B. [Ni(Me$_2$Ac$_2$Me$_2$malen)]		
Ni–N	1.844 (03)	C1–C5	1.512 (05)
Ni–O1	1.830 (02)	C2–C3	1.443 (05)
N–C3	1.297 (04)	C2–C7	1.485 (06)
N–C4	1.474 (05)	C3–C6	1.519 (11)
O1–C1	1.266 (05)	C4–C4'	1.511 (06)
O2–C7	1.203 (04)	C7–C8	1.495 (06)
C1–C2	1.388 (05)		
O1–Ni–N	93.5 (1)	C5–C1–C2	122.4 (4)
O1'–Ni–N	177.1 (1)	C3–C2–C1	121.4 (3)
N1'–Ni–N	89.1 (1)	C7–C2–C1	118.7 (3)
O1'–Ni–O1	83.6 (1)	C7–C2–C3	119.9 (3)
N1'–Ni–O1	177.3 (1)	C2–C3–N	122.7 (3)
C3–N–Ni	128.1 (2)	C6–C3–N	119.5 (7)
C4–N–Ni	112.0 (2)	C6–C3–C2	117.7 (6)
C4–N–C3	119.5 (3)	C4'–C4–N	108.9 (3)
C1–O1–Ni	129.0 (2)	C2–C7–O2	122.1 (4)
C2–C1–O1	124.8 (3)	C8–C7–O2	119.4 (4)
C5–C1–O1	112.7 (3)	C8–C7–C2	118.3 (3)

Table IV. Electrochemical Data[a] for the Nickel(II) Complexes in Acetonitrile

complex	$E_{1/2}(1)$, V $(\Delta E_p(1)$, V)	$E_{p,a}(2)$, V
[Ni(Me$_2$Ac$_2$H$_2$malen)]	0.72 (0.08)	1.4[b]
[Ni(Me$_2$Ac$_2$Me$_2$malen)]	0.61 (0.08)	1.1[b]
[Ni(Me$_2$H$_2$H$_2$malen)]	0.46[c]	
[Ni(Me$_2$H$_2$Me$_2$malen)]	0.40[c]	

[a] Potentials were measured at a platinum-disk working electrode in 0.1 M TBAT/CH$_3$CN vs. a Ag/0.1 M AgNO$_3$/CH$_3$CN reference electrode; the scan rate was 100 mV s^{-1}. [b] Broad. [c] Irreversible, so $E_{p,a}(1)$ is given.

For the complex [Ni(Me$_2$Ac$_2$H$_2$malen)], the acetyl groups are rotated out of the NiN$_2$O$_2$ plane by 15.6 and 18.0° for an average of 16.8°. The C=O functionalities are aligned toward the same (open) side of the ligand and twisted toward the same face. Except for the ethylene portion of the chelate, which is in the δ configuration and expected to have a low barrier of inversion,[15] the symmetry of the complex approximates C_s.

The acetyl groups in [Ni(Me$_2$Ac$_2$Me$_2$malen)] are also twisted out of the NiN$_2$O$_2$ plane, but in this case by the substantial amount

of 58.2°. As with [Ni(Me$_2$Ac$_2$H$_2$malen)], the carbonyl oxygens are closest to the open side of the ligand; however, the acetyl groups are now twisted toward opposite faces of the complex and are related by a C_2 axis. In fact, the entire complex has strict C_2 symmetry. We will address the significance of the difference between the acetyl rotation angles in the Discussion.

Electrochemistry. Cyclic voltammograms of the acetylated and deacetylated complexes were measured in 0.1 M TBAT/CH$_3$CN vs. a Ag/0.1 M AgNO$_3$/CH$_3$CN reference electrode. The results are summarized in Table IV. The acetylated complexes [Ni-(Me$_2$Ac$_2$H$_2$malen)] and [Ni(Me$_2$Ac$_2$Me$_2$malen)] show reversible

(14) For the acetyl rotation angle, we use the angle between the best least-squares planes for [C$_1$, C$_2$, C$_3$, C$_5$] and [C$_2$, C$_5$, C$_6$, O$_2$].[22] A similar definition applies for the other acetyl rotation angles.

(15) Purcell, K. F.; Kotz, J. C. *Inorganic Chemistry*; W. B. Saunders: Philadelphia, 1977; pp 636–637.
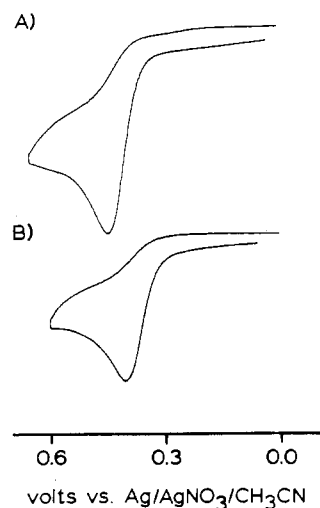
Figure 3. Cyclic voltammograms of (A) [Ni(Me$_2$H$_2$H$_2$malen)] and (B) [Ni(Me$_2$H$_2$Me$_2$malen)] in 0.1 M TBAT/CH$_3$CN with Ag/0.1 M AgNO$_3$/CH$_3$CN as the reference electrode. The concentration is 3 × 10^{-4} M in the complex for both voltammograms.

Table V. ^{13}C NMR Spectral Shifts for the Nickel(II) Complexes in Chloroform-d_1

complex	shifts,[a] ppm
[Ni(Me$_2$Ac$_2$H$_2$malen)]	194.6,[5] 188.6,[1] 159.9,[3] 114.4,[2] 58.6,[4] 28.9,[b] 28.4[b]
[Ni(Me$_2$Ac$_2$Me$_2$malen)]	204.2,[5] 176.9,[1] 164.2,[3] 117.9,[2] 54.4,[4] 33.5,[b] 24.8,[b] 20.0[b]
[Ni(Me$_2$H$_2$H$_2$malen)]	178.8,[1] 155.6,[3] 95.3,[2] 57.8,[4] 24.9[7]
[Ni(Me$_2$H$_2$Me$_2$malen)]	176.8,[1] 164.5,[3] 99.5,[2] 53.0,[4] 24.3,[b] 20.9[b]

[a] Superscript refers to carbon numbering scheme in structure III. [b] Methyl group; assignment ambiguous.

one-electron waves at 0.72 and 0.61 V, respectively. The peak-to-peak splitting of 80 mV observed for both couples is slightly larger than the theoretical 59 mV, as is often found in nonaqueous electrolytes.[16]

The reversible electrochemistry observed for the acetylated complexes is in sharp contrast to the results obtained for the deacetylated complexes. [Ni(Me$_2$H$_2$H$_2$malen)] and [Ni(Me$_2$H$_2$Me$_2$malen)] gave totally irreversible oxidations with peak potentials at 0.46 and 0.40 V, respectively. Although chemically irreversible, the oxidative scans were sharp and the peak potentials very reproducible. In fact, the shapes of the voltammograms for the two deacetylated complexes are very similar (Figure 3).

The acetylated complexes showed a second irreversible oxidation at higher potentials (E_p = 1.4 V for [Ni(Me$_2$Ac$_2$H$_2$malen)]; E_p = 1.1 V for [Ni(Me$_2$Ac$_2$Me$_2$malen)]). The observation of a reversible oxidative couple followed by an irreversible oxidation is strictly analogous to the results found for the nickel(II) cyclidene complexes.[17,18] For the deacetylated complexes, a second oxidation was observed; however, the intensity was decreased, presumably as a result of decomposition of the complex following the first oxidation.

^{13}**C NMR Spectroscopy.** ^{13}C NMR spectral data for the four NiN$_2$O$_2$ complexes in CD$_3$CN are given in Table V. The simple spectra obtained for these complexes are consistent with at least C_s or C_2 symmetry (vide supra). The most striking difference between the acetylated and deacetylated complexes is the low-field resonance for the acetylated complexes at around 200 ppm due to the carbonyl carbons.
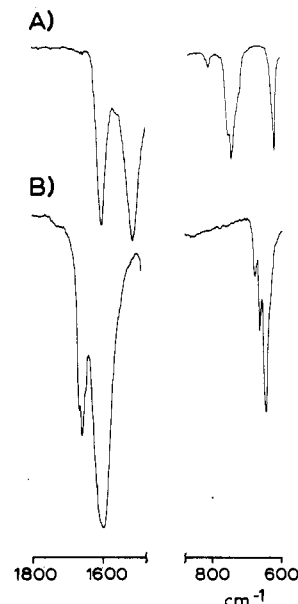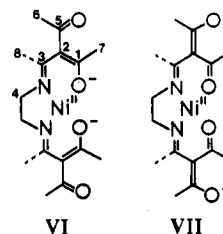
(16) Bailey, C. L.; Bereman, R. D.; Rillema, D. P.; Nowak, R. *Inorg. Chem.* **1984**, *23*, 3956–3960.

(17) Busch, D. H.; Jackels, S. C.; Callahan, T. J.; Grzybowski, J. J.; Zimmer, L. L.; Kojima, M.; Olszanski, D. J.; Schammel, W. P.; Stevens, J. C.; Holter, K. A.; Mocak, J. *Inorg. Chem.* **1981**, *20*, 2834–2844.

(18) Korybut-Daszkiewicz, B.; Kojima, M.; Cameron, J. H.; Herron, N.; Chavan, M. Y.; Jircitano, A. J.; Coltrain, B. K.; Neer, G. L.; Alcock, N. W.; Busch, D. H. *Inorg. Chem.* **1984**, *23*, 903–914.

Figure 4. Partial infrared spectra of (A) [Ni(Me$_2$H$_2$H$_2$malen)] and (B) [Ni(Me$_2$Ac$_2$H$_2$malen)] obtained as KBr pellets.

Infrared Spectroscopy. The infrared spectra of the deacetylated complexes are characteristic of complexes of this type.[19,20] The principal changes caused by acetylation are disappearance of the out-of-plane C—H wag[20] at roughly 750 cm^{-1}, coalescence of the C=C and C=N stretches, and appearance of a C=O stretch. These changes are shown in Figure 4 for the complexes [Ni(Me$_2$H$_2$H$_2$malen)] and [Ni(Me$_2$Ac$_2$H$_2$malen)]. Qualitatively, the differences in the infrared spectra for [Ni(Me$_2$H$_2$Me$_2$malen)] and [Ni(Me$_2$Ac$_2$Me$_2$malen)] are strictly analogous to that shown in Figure 4, except that the two acetylated complexes differ in their C=O stretching frequencies. The C=O stretches for the acetylated complexes [Ni(Me$_2$Ac$_2$H$_2$malen)] and [Ni(Me$_2$Ac$_2$Me$_2$malen)] occur at 1650 and 1660 cm^{-1}, respectively.

Discussion

The addition of two methyl groups to [Ni(Me$_2$Ac$_2$H$_2$malen)] to give [Ni(Me$_2$Ac$_2$Me$_2$malen)] has clearly had a profound effect on the orientation of the acetyl groups. The reason for this certainly lies with the steric bulk provided by the methyl groups, which force the acetyl groups to be rotated out of the NiN$_2$O$_2$ plane in [Ni(Me$_2$Ac$_2$Me$_2$malen)]. The rotation angle of the acetyl groups relative to the NiN$_2$O$_2$ plane is expected to be a significant factor in determining the relative contributions of the two principal resonance structures for the acetylated complexes (structures VI and VII).[21]

VI   VII

As the acetyl groups are twisted out of the NiN$_2$O$_2$ plane, the contribution of resonance structure VII is expected to decrease. Therefore, in the absence of other effects, resonance structure VII will contribute less to [Ni(Me$_2$Ac$_2$Me$_2$malen)] than it does to [Ni(Me$_2$Ac$_2$H$_2$malen)]. One obvious place to look for this effect

(19) (a) Kenney, J. W.; Nelson, J. H.; Henry, R. A. *J. Chem. Soc., Chem. Commun.* **1973**, 690. (b) Howells, P. N.; Kenney, J. W.; Nelson, J. H.; Henry, R. A. *Inorg. Chem.* **1976**, *15*, 124.

(20) Veno, K.; Martell, A. E. *J. Phys. Chem.* **1955**, *59*, 998.

(21) These resonance structures apply to both [Ni(Me$_2$Ac$_2$H$_2$malen)] and [Ni(Me$_2$Ac$_2$Me$_2$malen)], as indicated by the dashed line.

is in the relative bond lengths for the two acetylated complexes. Specifically, as one goes from [Ni(Me$_2$Ac$_2$H$_2$malen)] to [Ni-(Me$_2$Ac$_2$Me$_2$malen)], the increase in the acetyl rotation angle and concomitant decrease in the relative contribution of resonance structure VII are expected to result in a decrease in bond lengths C$_5$–O and C$_1$–C$_2$ and an increase in bond lengths C$_2$–C$_5$ and C$_1$–O.[22] The expected changes are observed (see Table III) for all but the C$_1$–O bond, but the differences are not significant with respect to the standard deviations of the bond lengths. Part of the problem is that the methyl groups used to impact steric bulk near the acetyl groups also make a complicating electronic contribution of their own (note that the greatest differences in bond lengths occur at the carbon that receives the extra methyl groups, i.e. C$_2$–C$_3$ and C$_3$–N). In order to address the effects of rotating the acetyl groups out of the NiN$_2$O$_2$ plane in [Ni-(Me$_2$Ac$_2$Me$_2$malen)], we need to know the electronic contributions of the added methyl groups.

Electrochemical Determination of Electronic Effects. Electrochemistry is a very useful technique for measuring the electronic contributions of ligand substituents to metal complexes of that ligand.[17,18,23,24] In our case, electrochemistry allows us to assess the electronic contributions of the added methyl groups in the absence of twisting effects for the acetyl groups by comparing the deacetylated complexes. Although oxidation of the deacetylated complexes is chemically irreversible, the scans are sharp and reproducible and show essentially the same shape when the concentrations of the complexes are the same. Therefore, the differences between the peak potentials of [Ni(Me$_2$H$_2$H$_2$malen)] and [Ni(Me$_2$H$_2$Me$_2$malen)] gives a reasonable estimate for the electronic effect of the extra methyl groups on [Ni-(Me$_2$H$_2$Me$_2$malen)]. The decrease in potential of 0.06 V as one goes from [Ni(Me$_2$H$_2$H$_2$malen)] to [Ni(Me$_2$H$_2$Me$_2$malen)] agrees with the expected increase in electron density on the complex upon replacing –H by –CH$_3$.

With an estimate for the electronic effect of the added methyl groups in hand, we may now consider the acetylated complexes. [Ni(Me$_2$Ac$_2$Me$_2$malen)] is 0.11 V easier to oxidize than [Ni-(Me$_2$Ac$_2$H$_2$malen)]. On the basis of the results for the deacetylated complexes, 0.06 V of this difference must be due to the electron-donating nature of the methyl groups relative to that of hydrogen. The remainder (0.11 V – 0.06 V = 0.05 V) must be due to the removal of the resonance contribution of structure VII as a result of rotating the acetyl groups out of the NiN$_2$O$_2$ plane. The result is to increase the electron density at the central oxygens and lower the redox potential by the observed 0.05 V.

Spectroscopic Evidence. If rotating the acetyl group out of the NiN$_2$O$_2$ plane has indeed had a resonance effect, this should be reflected in the spectroscopic properties of the two acetylated complexes. This is especially true for ^{13}C NMR spectroscopy, where an increase (decrease) in electron density on a particular carbon will lead to a decrease (increase) in chemical shift for that carbon. For the complexes of interest here, [Ni(Me$_2$Ac$_2$H$_2$malen)] and [Ni(Me$_2$Ac$_2$Me$_2$malen)], the most sensitive carbons are expected to be the carbons involved in carbon–oxygen bonds (carbons

1 and 5 in structure VI), since the oxygen atoms carry the formal charge in the resonance structures.

As one goes from [Ni(Me$_2$Ac$_2$H$_2$malen)] to [Ni-(Me$_2$Ac$_2$Me$_2$malen)], the acetyl carbonyl resonance is shifted from 194.6 to 204.3 ppm, suggesting a decrease in electron density at that carbon. Moreover, the resonance for the carbon atom attached to the chelating oxygen atom is shifted from 188.6 to 176.9 ppm, which suggests an increase in electron density. Both of these observations are consistent with a decrease in the contribution of resonance structure VII when the acetyl groups are turned out of the NiN$_2$O$_2$ plane. It is noteworthy that the chemical shift of the carbon atom attached to the chelating oxygen atom in [Ni(Me$_2$Ac$_2$Me$_2$malen)] is very close to the analogous resonances for the deacetylated complexes ([Ni(Me$_2$H$_2$H$_2$malen)], 178.8 ppm; [Ni(Me$_2$H$_2$Me$_2$malen)], 176.8 ppm), where electron density cannot be removed by such a resonance delocalization.

The observations described above cannot be explained by a simple inductive effect due to the added methyl groups on [Ni-(Me$_2$Ac$_2$Me$_2$malen)]. The inductive action accompanying the replacement of –H with –CH$_3$ would place more electron density on the complex. Thus, the inductive effect alone would shift the resonances attributable to both the carbon atom next to the chelating oxygen *and* the acetyl carbonyl upfield. The resonance effect is clearly important; however, the inductive effect of the added methyl groups may explain why the downfield shift of the carbonyl resonances (9.6 ppm) is less than the upfield shift of the resonances of the carbon atoms next to the chelating oxygen atoms (11.7 ppm) for [Ni(Me$_2$Ac$_2$H$_2$malen)] and [Ni-(Me$_2$Ac$_2$Me$_2$malen)].

The difference in carbonyl stretching frequencies for the acetylated complexes can also be explained in terms of a resonance effect involving the rotation angle of the acetyl groups. As the rotation angle is increased in going from [Ni(Me$_2$Ac$_2$H$_2$malen)] to [Ni(Me$_2$Ac$_2$Me$_2$malen)], the relative contribution from resonance structure VII will decrease. This is tantamount to increasing the double-bond character of the C to O bond, which should result in an increase in the C=O stretching frequency.[25] In fact, the carbonyl stretching frequency for [Ni(Me$_2$Ac$_2$Me$_2$malen)] is 10 cm^{-1} greater than that of [Ni(Me$_2$Ac$_2$H$_2$malen)].

Note again that this is the opposite of what would be expected from the purely inductive effect of adding two methyl groups to [Ni(Me$_2$Ac$_2$H$_2$malen)]. As stated earlier (and verified electrochemically), the additional methyl groups donate electron density to the complex, and the purely inductive effect would be to decrease the carbonyl stretching frequency.[25] The observed increase in carbonyl stretching frequency can only be explained in terms of a resonance mechanism.

From the accumulated results, it is concluded that the steric effect of the second methyl group in [Ni(Me$_2$Ac$_2$Me$_2$malen)] does indeed control the electronic interaction of the acetyl groups in this family of structures. The behavior is uniformly consistent over a variety of independent classes of measurement. In all cases, the effect is admittedly small; however, the uniformity of the results strongly supports the interpretation given.

(22) The subscripts here refer to the numbering scheme in structures III and VI. Note that, for [Ni(Me$_2$Ac$_2$H$_2$malen)], one should also consider the second half of the complex. This is not necessary for [Ni-(Me$_2$Ac$_2$Me$_2$malen)] since the halves are related by a C_2 axis.

(23) (a) Pillsbury, D. G.; Busch, D. H. *J. Am. Chem. Soc.* **1976**, *98*, 7836–7839. (b) Streeky, J. A.; Pillsbury, D. G.; Busch, D. H. *Inorg. Chem.* **1980**, *19*, 3148–3159.

(24) Busch, D. H.; Pillsbury, D. G.; Lovecchio, F. V.; Tait, A. M.; Hung, Y.; Jackels, S.; Rakowski, M. C.; Schammel, W. P.; Martin, L. Y. In *Electrochemical Studies of Biological Systems*; ACS Symposium Series 38; American Chemical Society: Washington, DC, 1977; pp 32–50.

(25) Silverstein, R. M.; Bassler, G. C.; Morrill, T. C. *Spectrometric Identification of Organic Compounds*, 4th ed.; Wiley: New York, 1981; p 117.